DOI: 10.7860/JCDR/2017/24165.9459

Original Article

Radiology Section

Thoracic Sarcoidosis: Imaging with High Resolution Computed Tomography

PEEYUSH KUMAR DHAGAT[1], SARVINDER SINGH[2], MEGHA JAIN[3], SATYENDRA NARAYAN SINGH[4], RAJAT KUMAR SHARMA[5]

ABSTRACT

Introduction: Sarcoidosis is a disease of unknown aetiology that primarily affects the lungs. Clinical and radiological findings with demonstration of non caseating granulomas on pathology is utilised for diagnosing the disease.

Aim: To assess and evaluate the features of thoracic sarcoidosis on High Resolution Computed Tomography (HRCT) chest.

Materials and Methods: A total of 40 (31 males and 9 females) cases of pulmonary sarcoidosis in a period of three years were included in this study. Patients underwent detailed clinical evaluation, imaging, Pulmonary Function Tests (PFT) and pathological confirmation of disease. Chest radiograph was obtained in all patients. HRCT was done on 16 slice Computed Tomography (CT) using 1 mm slice thickness and high spatial frequency algorithm for image re-construction. Images were viewed and evaluated using appropriate lung and mediastinal windows. The lymph nodes were classified as hilar and mediastinal with Maximum Short Axis Diameter (MSAD) more than 10 mm taken as cut-off for enlargement. Pulmonary opacities were classified as nodules (micronodules 1-4 mm and macronodules >5 mm), reticular opacities, fibrotic lesions, ground glass opacities and consolidations. Nodule distribution classified as perilymphatic centrilobular and random. Repeat scanning done on follow up or as clinically indicated.

Results: A total of five patients had Stage I disease, 24 patients had Stage II disease, eight patients had Stage III disease and three patients had stage IV disease. Mediastinal lymphdenopathy present in 29 patients. Bilateral hilar adenopathy was the predominant pattern seen in 22 patients. Lung parenchymal lesions excluding end stage disease noted in 32 patients. The characteristic HRCT lung parenchymal involvement of micronodules with a perilymphatic distribution was seen in 26 patients. HRCT features of predominant upper and middle lobe distribution seen in majority of patients. Documented atypical lesions and the characteristic features of end stage lung disease on HRCT noted in a small subset of patients. HRCT was superior to chest radiography for evaluating the features, pattern and distribution of the parenchymal lesions and mediastinal lymph nodes, for assessing the stage and activity of the disease and in aiding detection of subtle parenchymal lesions which are liable to be missed on conventional imaging.

Conclusion: Thoracic sarcoidosis can have varied presentations. HRCT is superior to conventional CT for the detection and characterisation of the lung parenchymal lesions.

Keywords: Lymphadenopathy, Necrosis, Pulmonary sarcoidosis

INTRODUCTION

Sarcoidosis is a disease of unknown aetiology which can affect any system in the body. Involvement of the lung parenchyma and mediastinal lymph nodes is the most common presentation of the disease and accounts for the majority of morbidity and mortality associated with the disease. Clinical and radiological findings with demonstration of non caseating granulomas on pathology are used for diagnosing the disease.

Imaging has a pivotal role in the diagnosis and follow up of the patients. Although chest radiography is often the initial imaging modality utilised, it has several limitations, including limited resolution for the detection of the parenchymal abnormalities and the mediastinal lymphadenopathy.

CT is more sensitive for the detection of parenchymal disease and adenopathy [1,2]. HRCT is more superior to conventional CT for detection and assessment of subtle parenchymal lesions and abnormalities of lung structures [3]. HRCT allows differentiation between active inflammation representing reversible disease from irreversible lung disease and fibrosis. Thus, it helps in prognosticating the disease and in guiding therapy. HRCT also helps in diagnosing the disease in patients with unusual radiographic findings and atypical presentations and is the investigation of choice for imaging the thorax [4].

Magnetic Resonance Imaging (MRI) is useful for evaluating the involvement of the myocardium in sarcoidosis. Radionuclide imaging, in particular 18F-Fluorodeoxyglucose Positron Emission Tomography (18FDG PET) may be helpful to assess activity of the disease [5]. Aim of this study is to assess and evaluate the features of lung parenchymal lesions and mediastinal lymph nodes in thoracic sarcoidosis on HRCT.

MATERIALS AND METHODS

A total of 40 pathologically confirmed cases of pulmonary sarcoidosis who reported to our institution during a three year period (2014 to 2016) were included in this study. Ethical committee clearance was obtained prior to the study and consent was obtained from all patients included in the study. All patients underwent detailed clinical evaluation, PFT and flexible bronchoscopy. Tissue for pathological evaluation was obtained by Transbronchial Needle Aspiration (TBNA), transbronchial biosy and image guidance.

Chest radiograph was obtained in all patients. The disease was staged with the Siltzbach classification into five stages. Stage 0, with a normal chest radiography; Stage 1, with mediastinal lymphadenopathy; Stage 2, with lymphadenopathy and parenchymal lung disease; Stage 3, with parenchymal lung lesions only; and Stage 4, with end stage pulmonary fibrosis [1,2].

HRCT was done on 16 slice CT (Siemens Somaton Emotion). Technical protocols utilised were: slice thickness: 1 mm, scan time:

5 seconds, kV: 130, mAs: 100, collimation: 1.5-3 mm, matrix size 768x768, FOV: 300 mm. High spatial frequency algorithms was used for reconstruction of images. Contrast enhanced scans were done in some patients in order to better evaluate the mediastinal lymphadenopathy. The scans were obtained in end inspiration. Appropriate windowing was done using lung and mediastinal windows.

The lymph nodes were classified as hilar and mediastinal. The criterion for enlargement was taken as more than 10 mm Maximum Short Axis Diameter (MSAD) for the lymph nodes. Pulmonary opacities were classified as nodules, reticular opacities, fibrotic lesions, ground glass opacities and patchy and confluent consolidations. Nodules were classified as micronodules (1-4 mm) and macronodules (>5 mm). The margins of the nodules (smooth/irregular) were noted. The distribution of the nodules was noted and classified as perilymphatic (along the peribronchovascular interstitium, subpleural, along the interlobular septa), centrilobular and random. The predominant distribution of the lesions in the various zones of the lungs (upper, middle or lower zone) was recorded. Repeat scanning was performed on patients on follow up or on those with worsening of symptoms as clinically indicated.

RESULTS

There were 31 males and 9 females. Most were in 30-50 year age group. Dry cough was the most common symptom. Majority had Stage II disease [Table/Fig-1].

Age Group (years)	Frequency (%)
0-10	0(0.0)
10-20	0(0.0)
20-30	05(12.5)
30-40	17(42.5)
40-50	14(35.0)
50-60	04(10.0)
Gender	
Male	31(77.5)
Female	09(22.5)
Stage	
O	0(0.0)
I	05(12.5)
II	24(60.0)
III	08(20.0)
IV	03(7.5)
Total	**40(100.0)**

[Table/Fig-1]: Distribution of study participants based on baseline characteristics.

A total of 29 patients had presence of mediatinal lymphdenopathy [Table/Fig-2]. Lymph nodes were present in the hilar, pre and paratracheal, AP window, prevascular and subcarinal regions. Bilateral hilar adenopathy was the most common finding seen in 22 patients [Table/Fig-3]. Paratracheal adenopathy especially on the right was seen in 15 patients. The size of the lymph nodes varied from 10 mm to 4.8 cm. Presence of conglomerate lymph nodes was seen in 11 patients. Necrosis present as low attenuating areas within the lymph nodes was not seen in any case. No retrocrural, internal mammary or significant axillary adenopathy was noted. A total of five patients had calcifications in the lymph nodes. Three patients had punctuate/nodular and two patients had egg shell calcification in the lymph nodes [Table/Fig-4].

Mediastinal Lymph Nodes (n=29)			
Bilateral hilar adenopathy 22 patients (76%)	Calcification n = 05 patients (17%)	Discrete nodes n=18 (62%)	Conglomerate nodes n= 11 (34%)

[Table/Fig-2]: Pattern and distribution of mediasinal lymphadenopathy.

[Table/Fig-3]: Axial non contrast (a) and contrast (b) CT images shows typical bilateral symmetrical hilar adenopathy (bold arrow) and subcarinal adenopathy (curved arrow).

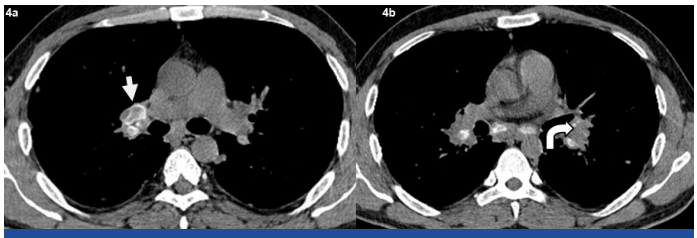

[Table/Fig-4]: Axial non contrast CT images shows (a) typical eggshell calcification in the right hilar lymph nodes (bold arrow). (b) punctuate and nodular calcifications seen in the left hilar lymph nodes (curved arrow).

A total of 32 patients had lung parenchymal lesions excluding end stage lung disease [Table/Fig-5]. The lung parenchymal findings were classified as being typical or atypical. The most common typical finding seen in 26 patients was micronodular opacities (1-3 mm in size) in a perilymphatic distribution. Perilymphatic distribution included nodules in the peribronchovascular distribution, subpleural regions and nodules along the interlobular septum. Perilymphatic distribution was most commonly appreciated in the parahilar regions and was seen as thickening and nodularity of the peribronchovascular interstitium and in the subpleural locations adjacent to the fissures [Table/Fig-6]. Areas of coalescing of the micronodules into larger nodules of varying sizes were seen in most cases [Table/Fig-7]. Atypical findings were noted in six patients. These atypical findings included patchy ground glass opacities [Table/Fig-8], focal consolidations and confluent conglomerate opacities [Table/Fig-9]. Findings of mosaic attenuation and air trapping were seen in three patients. Predominant involvement of the upper and middle zones was seen in 31 patients. In nine patients, the lesions were found involving both lungs in a diffuse manner [Table/Fig-10,11].

Lung lesions (n=35)		
Parenchymal lesions excluding end stage disease n= 32 (91.5%)		End stage disease with fibrosis and traction brochiectasis n= 03 (8.5%)
Typical pattern with perilymphatic distribution n= 26 (81%)	Atypical findings of patchy ground glass, consolidations etc n= 06 (19%)	

[Table/Fig-5]: Pattern and distribution of lung lesions.

End stage lung disease was seen in three patients with presence of fibrosis, reticulation and traction bronchiectasis [Table/Fig-12]. Cardiac sarcoidosis with focal thining and bowing of the interventricular septum was seen in one patient which was subsequently confirmed on MRI [Table/Fig-13,14]. No patient had evidence of pleural effusion, pleural plaques or pleural calcification. No cavitatory lesions were seen. No patient in this study had any upper abdominal pathology in the visualised images.

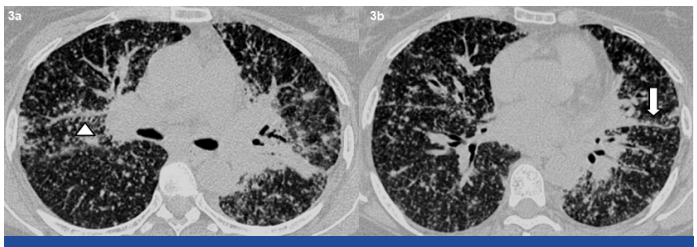

[Table/Fig-6]: Axial high resolution CT images shows typical perilymphatic distribution of micronodules in the peribronchovascular distribution (arrowhead) (a) and along the fissures. (bold arrow) (b).

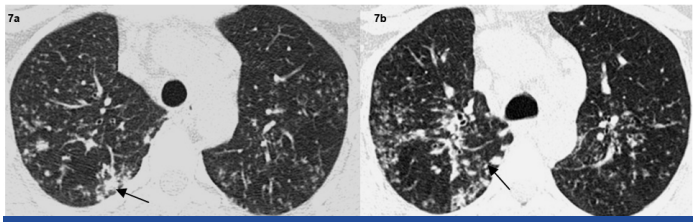

[Table/Fig-7]: Axial high resolution CT images show macronodules in the right lung(arrows) (a,b).

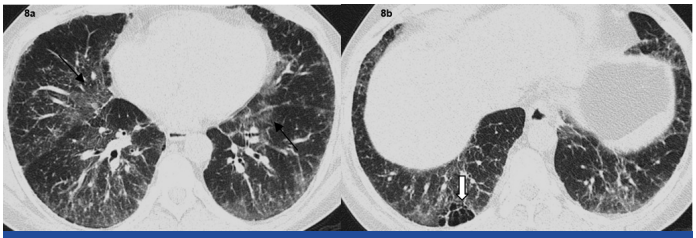

[Table/Fig-8]: Axial high resolution CT images show (a) patchy ground glass opacification in both lungs (arrows). (b) Focal air trapping seen in right lower lobe (Bold arrow).

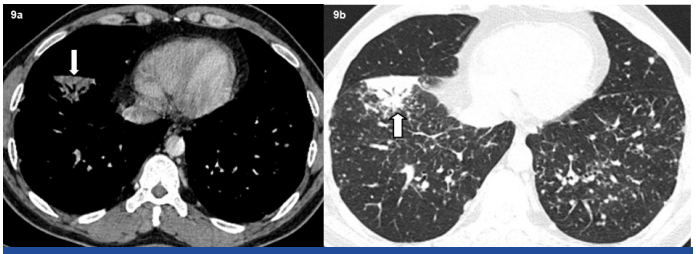

[Table/Fig-9]: Axial high resolution CT images show subsegmental consolidation with air bronchograms (bold arrow).

Distribution of lesions n=40	
Upper and middle zones n= 31 (78%)	Diffuse distribution n= 09 (22%)

[Table/Fig-10]: Distribution of lung nodules.

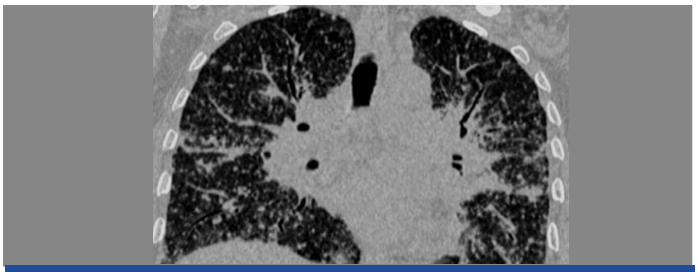

[Table/Fig-11]: Coronal re-formatted image shows diffuse distribution of the lung nodules in both lung fields in a typical perilymphatic distribution.

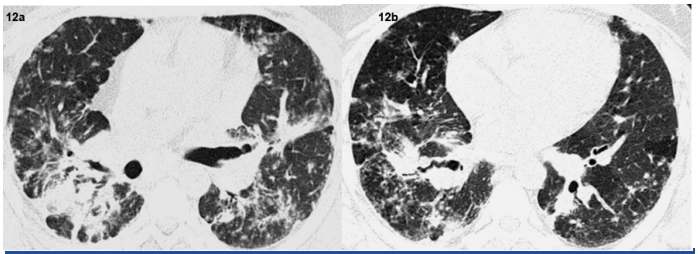

[Table/Fig-12]: Axial high resolution CT images show end stage lung disease with fibrosis traction bronchiectasis, architectural distortion and mosaic attenuation.

[Table/Fig-13]: Representative axial contrast enhanced CT scan image in mediastinal window (a), TRUFI (b) TIRM (c) MR images shows thinning and bowing of the interventricular septum towards the right side (arrow).

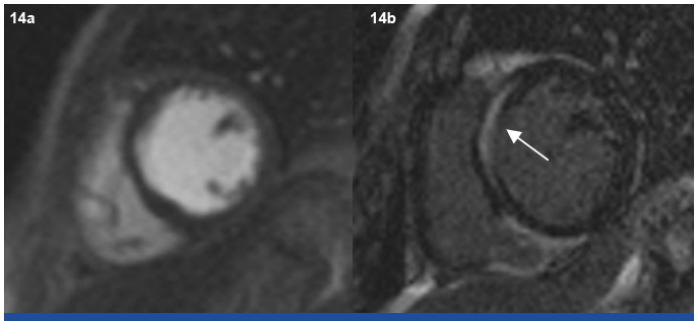

[Table/Fig-14]: Post-contrast cardiac MR images (short axis view) show no focal area of myocardial perfusion deficit after contrast administration (a). On delayed image, contrast enhancement of the septum seen (arrow) (b).

DISCUSSION

Sarcoidosis is a disease that can involve multiple systems. Thoracic involvement is the most common presentation and accounts for most of the symptoms. Most patients (40-50%) have stage I disease i.e., present with mediastinal lymphadenopathy. Stage II disease with lymphadenopathy and pulmonary involvement is the next common presentation seen in 25- 30% patients [1,3,4]. In this study, 60% patients (n=24) had stage II disease and 12.5% (n=5) had stage I disease. This variation is probably incidental and is likely due to the smaller sample size of this study.

Predominant involvement of hilar and right paratracheal lymph nodes is seen in 50-90% of the patients with mediastinal adenopathy in thoracic sarcoidosis [1,5-7]. The lymphadenopathy in sarcoidosis is usually non-necrotic, bilateral and symmetrical. Nodes are also seen in the prevascular region, AP window and subcarinal regions. In this study, 72.5% (n=29) of the patients had presence of mediastinal lymphadenopathy. Amongst them, 76% (n=22) had involvement of bilateral hilar lymph nodes and 15 patients in addition to hilar nodes had paratracheal lymphadenopathy. Patients also had nodes in the prevascular, sub aortic and subcarinal regions. Conglomerate lymph nodes were seen in 38% (n=11) patients. Nodal calcification is fairly frequent in long standing disease and the pattern can be amorphous, punctuate or eggshell [1]. Two patients (7%) had peripheral egg shell calcification in the hilar nodes. This finding has been reported in sarcoidosis although it may be seen in other conditions such as silicosis. The remaining three patients had a nodular/punctate pattern of calcification. Necrosis was not noted in the mediastinal nodes in this study. The characteristic predominant involvement of bilateral hilar and paratracheal lymph nodes associated with their typical non necrotic character, pattern of calcification and distribution found on HRCT in this study are in concurrence with findings of sarcoidosis in the published literature [8-10].

Perilymphatic distribution of the micronodules is the hall mark of sarcoidosis. The nodules are usually sharply defined, have a bilateral and generally symmetrical distribution and mainly involve the upper and mid zones [1,6,11]. The nodules are most frequently seen along the peribronchovascular interstitium and in the subpleural locations. Interlobular septal nodules are seen less frequently. The nodules frequently coalesce into larger nodules [3,12,13]. Lung parenchymal lesions excluding end stage disease was seen in 80% (n=32) of the patients. Presence of micronodules in a perilymphatic distribution, mainly along the peribronchovascular and subpleural distribution with frequent coalescing of nodules was the most predominant finding on HRCT in this study as seen in 65% (n=26) patients. These findings of predominantly micro nodules, their characteristic features, their typical perilymphatic pattern of distribution in the lung parenchyma, the lobar predominance, their tendency for coalescing, and their progression to end stage lung disease in a subset of patients, seen in this study are in concurrence with findings of sarcoidosis in the published literature [12,14,15].

Atypical lung parenchymal lesions were noted in a subset of

patients 15% (n=06). These atypical lesions consisted of large pulmonary nodules and masses, patchy air space consolidations, patchy ground glass opacities and areas of air trapping and mosaic attenuation. These opacities represent confluent and coalescing nodules in the interstitium or the acini of the lung parenchyma and are seen in 10 to 40% of patients and are often superimposed on the background of the interstitial nodules [1,13,16]. Air trapping is a non-specific finding which may be seen in a number of patients. Mosaic attenuation pattern indicates small airway involvement by granulomas or fibrosis [17,18].

Fibrosis, bullae, cicatricial emphysema and subpleural honey combing represent advanced stage of sarcoidosis and usually involve the upper and mid zones of the lungs with relative sparing of the bases [1,5]. Extensive fibrosis with traction bronchiectasis was seen in 7.5 % (n=03) patients with end stage lung disease. Cavitatory parenchymal lesions, miliary nodules and pleural involvement are uncommon in sarcoidosis [11,19]. No such findings were noted in this study.

One patient was found to have focal thinning and bowing of the interventricular septum. Cardiac MRI showed delayed endocardial enhancement, features consistent with cardiac sarcoidosis. However, similar enhancement can be seen in other forms of myocarditis [20]. The patient also had the classical nodules in a perilymphatic distribution in the lung parenchyma.

HRCT utilises thin sections and high frequency reconstruction algorithms to generate images and this results in better characterisation and definition of the abnormalities of the lung parenchyma. HRCT is superior to conventional CT for assessing subtle parenchymal lesions and helps to differentiate active lesions from end stage disease [1,21].

LIMITATION

A larger sample volume with a longer follow up would have accrued more data with better comparison with the established studies.

CONCLUSION

HRCT is the modality of choice for evaluating the features of thoracic sarcoidosis. It depicts the characteristic features of the parenchymal nodules and lesions, their distribution, the associated changes and atypical features very accurately. It also helps in guiding the appropriate therapy by differentiating active lesions from irreversible fibrosis.

REFERENCES

[1] Criado E, Sánchez M, Ramírez J, Arguis P, DeCaralt TM, Perea RJ, et al. Pulmonary sarcoidosis: Typical and atypical manifestations at high resolution computed tomograhpy with pathologic correlation. RadioGraphics. 2010;30:1567–86.
[2] Webb WR, Higgins CB. Thoracic imaging. 2nd Edition. Philadelphia: Lippincott Williams & Wilkins; 2011.
[3] Nunes H, Brillet PY, Valeyre D, Brauner MW, Wells AU. Imaging in sarcoidosis. Semin Respir Crit Care Med. 2007;28:102-20.
[4] Silva M, Nunes H, Valeyre D, Sverzellati N. Imaging of sarcoidosis. Clin Rev Allergy Immunol. 2015;49(1):45-53.
[5] Wessendorf TE, Bonella F, Costabel U. Diagnosis of sarcoidosis. Clin Rev Allergy Immunol. 2015;49(1):54-62.
[6] Avital M, Halpern IH, Deeb M, Izbicki G. Radiological findings in sarcoidosis. IMAJ. 2008;10:572-74.
[7] Reich JM. Mortality of intrathoracic sarcoidosis in referral vs population-based settings: influence of stage, ethnicity, and corticosteroid therapy. Chest. 2002;121(1):32–39.
[8] Nunes H, Uzunhan Y, Gille T, Lamberto C, Valeyre D, Brillet PY. Imaging of sarcoidosis of the airways and lung parenchyma and correlation with lung function. Eur Respir J. 2012;40:750–65.
[9] Morawiec E, Hachulla-Lemaire AL, Chabrol J, Remy-Jardin M, Wallaert B. Venoatrial compression by lymphadenopathy in sarcoidosis. Eur Respir J. 2010;35:1188–91.
[10] Lynch JP, Ma YL, Koss MN, White ES. Pulmonary sarcoidosis. Semin Respir Crit Care Med. 2007;28:53-74.
[11] Ortega IH, Gonzalez LL. Update thoracic sarcoidosis. Radiologia. 2011;53(5):443-48.
[12] Koyama T, Ueda H, Togashi K, Umeoka S, Kataoka M, Nagai S. Radiologic manifestations of sarcoidosis in various organs. RadioGraphics. 2004;24(1):87–104.
[13] Al Jahdali H, Rajiah P, Koteyar SS. Atypical radiological manifestations of thoracic sarcoidosis: A review and pictorial essay. Annals of Thoracic Medicine. 2013;8(4):186-96.
[14] Malaisamy S, Dalal B, Bimenyuy C, Soubani AO. The clinical and radiologic features of nodular pulmonary sarcoidosis. Lung. 2009;187:9–15.
[15] Baughman RP, Shipley R, Desai S, Drent M, Judson MA, Costabel U, et al. Changes in chest roentgenogram of sarcoidosis patients during a clinical trial of infliximab therapy: Comparison of different methods of evaluation. Chest. 2009;136:526–35.
[16] Armengol G, Bernet J, Lahaxe L, Lévesque H, Marie I. Uncommon manifestation revealing sarcoidosis. Rev Med Interne. 2009;30:53-57.
[17] Bartz RR, Stern EJ. Airways obstruction in patients with sarcoidosis: expiratory CT scan findings. J Thorac Imaging. 2000;15(4):285–89.
[18] Davies CW, Tasker AD, Padley SP, Davies RJ, Gleeson FV. Air trapping in sarcoidosis on computed tomography: Correlation with lung function. Clin Radiol. 2000;55(3):217–21.
[19] Martin SG, Kronek LP, Valeyre D, Brauner N, Brillet PY, Nunes H, et al. High-resolution computed tomography to differentiate chronic diffuse interstitial lung diseases with predominant ground-glass pattern using logical analysis of data. Eur Radiol. 2010;20:1297–310.
[20] Slater GM, Rodriguez ER, Lima JA, Bluemke DA. A unique presentation of cardiac sarcoidosis. AJR Am J Roentgenol. 2003;180:173-89.
[21] Keijsers RG, Veltkamp M, Grutters JC. Chest imaging. Clin Chest Med. 2015;36(4):603-19.

PARTICULARS OF CONTRIBUTORS:
1. Associate Professor, Department of Radiology, Base Hospital, Delhi Cantt, New Delhi, India.
2 Associate Professor, Department of Respiratory Medicine, Base Hospital, Delhi Cantt, New Delhi, India.
3 Senior Resident, Department of Radiology, Army College of Medical Science, New Delhi, India.
4 Associate Professor, Department of Radiology, Base Hospital, Delhi Cantt, New Delhi, India.
5 Assistant Professor, Department of Radiology, Base Hospital, Delhi Cantt, New Delhi, India.

NAME, ADDRESS, E-MAIL ID OF THE CORRESPONDING AUTHOR:
Dr. Peeyush Kumar Dhagat,
Col Peeyush K Dhagat Senior Advisor (Radiology), Department of Radiology, Base Hospital,
Delhi Cantt, New Delhi-110010, India.
E-mail: peeyushdhagat@gmail.com

FINANCIAL OR OTHER COMPETING INTERESTS: None.

Date of Submission: **Sep 15, 2016**
Date of Peer Review: **Oct 18, 2016**
Date of Acceptance: **Nov 01, 2016**
Date of Publishing: **Feb 01, 2017**